

Investigation of Triplet States of 2-(2'-Hydroxyphenyl)benzothiazole and 2-(2'-Hydroxyphenyl)benzoxazole by Transient Absorption Spectroscopy and ab Initio Calculations

Shin-ichi Nagaoka,* Akinori Itoh, and Kazuo Mukai

Department of Chemistry, Faculty of Science, Ehime University, Matsuyama 790, Japan

Umpei Nagashima

Department of Information Sciences, Faculty of Science, Ochanomizu University, Otsuka, Bunkyo-ku, Tokyo 112, Japan

Received: May 24, 1993; In Final Form: August 12, 1993*

Properties of the $^3(\pi, \pi^*)$ states of 2-(2'-hydroxyphenyl)benzothiazole (HBT) and 2-(2'-hydroxyphenyl)benzoxazole (HBO) were investigated by means of transient absorption spectroscopy and ab initio calculations. When the volume fraction of ethanol in a mixed solvent of toluene and ethanol is small, the intramolecularly proton-transferred *cis*-keto form of HBT predominates over the intermolecularly hydrogen-bonded *trans*-enol form in the triplet state. However, when the volume fraction of ethanol becomes large, the relative composition is reversed. The triplet species of HBO at 10 μ s after photoexcitation contain a *cis*-enol form in both nonpolar and alcoholic solvents. For HBO, the *cis*-keto form produced immediately after photoexcitation is partly converted to the intramolecularly hydrogen-bonded *cis*-enol form in the triplet state within 10 μ s. Interpretation of the solvent effect is made on the basis of the ab initio calculations for the ground state. The difference in solvent effect between HBT and HBO can be explained in terms of the hydrogen bonding involving the sulfur or oxygen atom at the 1-position. The results of the ab initio calculations for the triplet state show that the stable triplet species of HBT and HBO can be regarded as a kind of *cis*-keto form. This result can be explained by considering the π electron nodal pattern of the wave function in the lowest $^3(\pi, \pi^*)$ state.

Introduction

The photoinduced intramolecular proton transfer of hydrogen-bonded molecules is a topic of current interest.^{1–6} It is a very simple chemical process and is of great interest in view of its use as a polymer-protecting agent⁷ and the possibilities of making a proton-transfer laser⁸ and an information storage device at the molecular level.⁹ Accordingly, we have investigated the dynamic processes of various excited states of *o*-hydroxybenzaldehyde (OHBA) in detail.^{7,10–17}

In previous studies concerning intramolecular proton transfer, attention was mainly focused on the lowest excited singlet states (S_1 states). Only a few systems have been studied on the triplet states of the intramolecularly hydrogen-bonded molecules. In a previous paper,¹⁷ we studied the spectroscopy and dynamics in the lowest $^3(\pi, \pi^*)$ states of OHBA and related molecules by means of time-resolved electron paramagnetic resonance (TR-EPR).

On the other hand, the mechanism of the photoinduced proton transfer of 2-(2'-hydroxyphenyl)benzothiazole (HBT) and 2-(2'-hydroxyphenyl)benzoxazole (HBO) has been extensively investigated in recent years.^{18–45} The main species in the ground states (S_0 states) of HBT and HBO are intramolecularly hydrogen-bonded *cis*-enol forms (Figure 1) in nonpolar solvents. In the lowest $^3(\pi, \pi^*)$ states of HBT and HBO, proton-transferred *cis*-keto forms (Figure 1) are considered to be stabilized in the intramolecularly hydrogen-bonded species by the node of the wave function.^{13–15,46,47} In previous papers, Tero-Kubota et al.⁴¹ and we⁴² studied the spectroscopy and dynamics in the triplet states of HBT and HBO by means of TREPR.

In the present paper, we have tried to make a detailed investigation of the solvent effects and the stable species in the triplet states of HBT and HBO. We have, thus, measured the transient absorption spectra of HBT, HBO, 2-(2'-methoxyphenyl)benzothiazole (MBT), 6-[3-methyl-2(3*H*)-benzothiazolylidene]cyclohexa-2,4-dienone (NBT), and 2-(2'-hydroxy-6'-methyl-

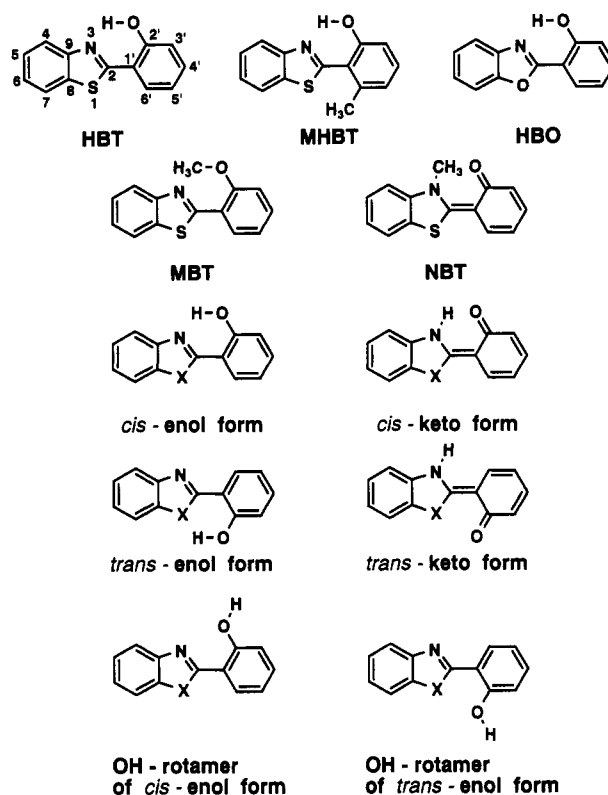


Figure 1. Molecular structures of MBT, NBT, and enol and keto forms of HBT and HBO, together with numbering system for atoms used in the present work.

phenyl)benzothiazole (MHBT). First, we tried to confirm the molecular structures in the lowest $^3(\pi, \pi^*)$ states of HBT and HBO in nonpolar and alcoholic solvents experimentally by comparison with the spectra of MBT and NBT. Secondly, by the use of MHBT we studied the reason for the difference in solvent effect between HBT and HBO. Thirdly, we tried to

* Abstract published in *Advance ACS Abstracts*, October 15, 1993.

determine the molecular structure of the transient species of HBT obtained after photoexcitation at room temperature experimentally.

However, it is difficult to determine the properties of the triplet states of HBT and HBO unambiguously by means of TREPR and transient absorption spectroscopy alone. In order to obtain further information about the triplet state, it is desirable to perform nonempirical molecular-orbital (MO) calculations at a reliable level of theory. In the present paper, interpretation of the solvent effects in the transient absorption spectra of HBT and HBO has been made on the basis of *ab initio* calculations for the S_0 states. The optimized structures in the lowest $^3(\pi, \pi^*)$ states of HBT and HBO were obtained, and the exact nature of the proton transfer was discussed on the basis of the calculated results. The molecular structures of MBT, NBT, and the enol and keto forms of HBT and HBO are shown in Figure 1, together with the numbering system for the atoms used in the present work.

Experimental Section

Commercially obtained HBT and HBO were purified by repeated recrystallization from ethanol (EtOH). EtOH used as a solvent was refluxed over CaO for 12 h and then distilled twice. CaO was previously heated at high temperature for 6 h. Toluene (Tol), diethyl ether (DEE), and isopentane (IP) used as solvents were refluxed over Na or NaH for 12 h and then distilled twice. EtOH and DEE were mixed with Tol and IP, respectively, to obtain stable glass matrixes (EtOH + Tol and DEE + IP, respectively).

MBT was synthesized according to a procedure similar to that reported by Nakagaki et al.¹⁹ HBT (2.3 g) was dissolved in 2 N aqueous NaOH solution (30 mL), and $(\text{CH}_3)_2\text{SO}_4$ (1.3 g) was added dropwise. The precipitated MBT was separated by filtration and was purified by column chromatography on silica gel with CH_2Cl_2 . The residue obtained after evaporation was recrystallized from petroleum ether, giving white crystals (mp 106–108 °C). In the ^1H NMR spectrum of HBT in CDCl_3 , the peak at $\delta = 12.04$ ppm was assigned to the hydrogen atom of the OH group. However, in MBT, there were no peaks around 12 ppm, and instead a peak was seen at $\delta = 4.03$ ppm, which was assigned to the hydrogen atoms of the OCH_3 group. The most abundant peak in the mass spectrum was that of $m/e = 241$, which was assigned to the parent ion of MBT. The first absorption band showed the maximum at 320 nm in DEE + IP. The fluorescence spectrum showed a peak at 355 nm in DEE + IP, and the Stokes shift was small.

NBT was synthesized according to a procedure similar to that reported by Williams et al.^{18,48} HBT (4.5 g) was dissolved in $(\text{CH}_3)_2\text{SO}_4$ (2.5 g), and the solution was heated at 120 °C (oil bath) for 30 min. The solution was allowed to cool to room temperature. The produced 2-(2'-hydroxyphenyl)-3-methylbenzothiazolium methyl sulfate was washed with a small amount of dry DEE and was dissolved in water (20 mL). The solution was made alkaline with 10% aqueous NaOH solution. The precipitated NBT was separated by filtration and was purified by column chromatography on silica gel with methanol. After removal of the solvent, the orange powder was obtained (mp 139–142 °C). In the ^1H NMR spectrum in CD_3OD , there were no peaks around 12 ppm, and instead a peak was seen at $\delta = 4.30$ ppm, which was assigned to the hydrogen atoms of the CH_3 group bonded to N_3 . The most abundant peak in the mass spectrum was that of $m/e = 240$, and the one of $m/e = 241$ followed this. The peak of $m/e = 241$ was assigned to the parent ion of NBT. Since the solubility of NBT in EtOH + Tol was very small, we used DEE + IP as the solvent for NBT. The first absorption band showed the maximum at 461 nm in DEE + IP. The fluorescence spectrum showed a peak at 468 nm in DEE + IP, and the Stokes shift was small.

MHBT was synthesized from 2-hydroxy-6-methylbenzaldehyde according to a procedure similar to that reported by Cossey

et al.⁴⁹ 2-Hydroxy-6-methylbenzaldehyde was prepared from OHBA.⁵⁰ A mixture of 2-hydroxy-6-methylbenzaldehyde (2.46 g) and 2-aminobenzenethiol (2.5 g) in excess nitrobenzene (20 g) was refluxed for 3 h. Nitrobenzene was an oxidizing agent. The solution was allowed to cool to room temperature. The precipitated MHBT was separated by filtration and was washed with a small amount of EtOH. Recrystallization from EtOH gave white needles (mp 132–134 °C). In the ^1H NMR spectrum in CCl_4 , peaks were seen at $\delta = 2.32$, 6.7–8.0, and 12.32 ppm, which were assigned to the three hydrogen atoms of the CH_3 group at the 6'-position, seven hydrogens of the aromatic rings, and one hydrogen of the hydroxy group, respectively. The most abundant peak in the mass spectrum was that of $m/e = 241$, which was assigned to the parent ion of MHBT. The first absorption band showed the maximum at 340 nm in EtOH + Tol (1:9 volume ratio). The fluorescence spectrum showed a peak at 510 nm in EtOH + Tol (1:9 volume ratio), and the Stokes shift was very large.

Transient absorption spectra, steady-state absorption spectra, and fluorescence spectra were obtained with a Unisoku USP-500 pulse-flush spectrometer, a Shimadzu UV-2100S spectrophotometer, and a Shimadzu RF-5000 spectrofluorophotometer, respectively. The concentrations of samples were 10^{-4} to 10^{-3} M in the measurements of the transient absorption spectra. A pyrex cell of test-tube type was usually used in the experiments at 77 K. The transient absorption spectra obtained with a 1-cm square quartz cell were essentially the same as those obtained with a pyrex cell of test-tube type. The transient absorption spectra were obtained at 10 μs after photoexcitation. Unless otherwise noted, lifetimes of transient species were longer than the longer limit of detection in our apparatus (1 ms).

Calculation Method and Procedure

Pariser–Parr–Pople Method. The wavelengths of the triplet-triplet absorption (T–T absorption) of the hydrogen-bonded enol and keto forms of HBT and HBO were calculated using the semiempirical Pariser–Parr–Pople-type (PPP-type) MOs. The wavelengths of the T–T absorption calculated with the PPP method agree well with the experimental ones.^{51,52} We used a procedure similar to that reported previously.^{17,42,53,54} Two-center electron repulsion integrals and two-center core integrals (β_s) were evaluated by using the Ohno–Klopman-type^{55–57} and Wolfsberg–Helmholtz-type⁵⁸ approximations, respectively. β for benzene was assumed to be -2.39 eV. The ionization potential (IP) and electron affinity (EA) given by Hinze, Jaffé, Dewar, and Morita^{59,60} do not satisfactorily reproduce the observed trend of the experimental results as reported previously.⁵⁴ Accordingly, we used alternative IP and EA values:⁵⁴ for the O_1 atom of HBO and the O_2 atoms of the enol forms of HBT and HBO, the IP and EA were taken as 32.93 and 17.70 eV, respectively; for the N_3 atoms of the keto forms of HBT and HBO, the IP and EA were taken as 26.46 and 14.12 eV, respectively; for the S_1 atom of HBT, the IP and EA were taken as 22.64 and 12.70 eV, respectively.

In the π electron MO treatment, the effect of hydrogen bonding is conveniently treated by changing the Coulomb parameter α .^{17,42,53} The hydrogen-bonding formation is expected to increase and decrease the α values for the O_2 and N_3 atoms in the enol forms of HBT and HBO, respectively. It also increases and decreases those for the N_3 and O_2 atoms in the keto forms, respectively. The symbol $\Delta\alpha$ is used to designate the change in α . We assumed that the $|\Delta\alpha|$ values for the O_2 and N_3 atoms of a molecule are equal to each other, as in the case of methyl salicylate.¹⁷ From the calculated results of the zero-field splittings in the triplet state, the $|\Delta\alpha|$ values for the enol and keto forms were determined to be 1 and 2 eV, respectively.⁴²

Ab Initio Method. *Ab initio* calculations for HBT and HBO were carried out with the Gaussian 88 program.⁶¹ The basis set

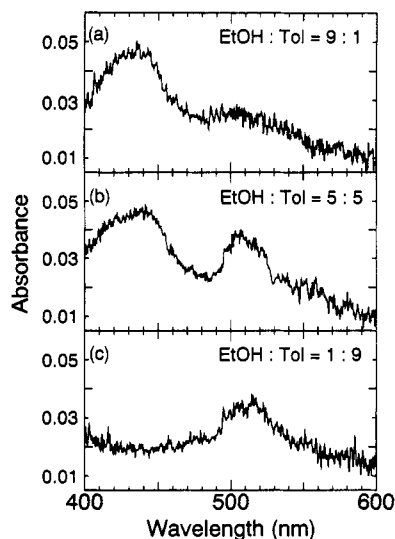


Figure 2. Transient absorption spectra of HBT obtained at 10 μ s after photoexcitation in EtOH + Tol of various volume ratios at 77 K. (a) EtOH : Tol = 9:1. (b) 5:5. (c) 1:9.

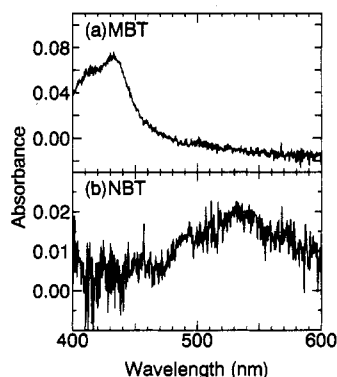


Figure 3. (a) Transient absorption spectrum of MBT in EtOH + Tol (1:9 volume ratio). (b) Transient absorption spectrum of NBT in DEE + IP (1:1 volume ratio). These spectra were obtained at 10 μ s after photoexcitation at 77 K.

used in the present calculations is STO-3G, which reproduces the experimental results fairly well.⁶² The restricted Hartree-Fock (RHF) and the unrestricted Hartree-Fock (UHF) schemes were adopted in the self-consistent-field (SCF) calculations for the S_0 and triplet states, respectively. The geometry optimization was performed under the constraint of C_s symmetry by the energy gradient method.

Results and Discussion

Transient Absorption. Figure 2 shows the transient absorption spectra of HBT in EtOH + Tol of various volume ratios at 77 K. Two peaks can be seen around 430 and 510 nm. The latter wavelength is close to that of the T-T absorption maximum of HBT obtained in 3-methylpentane at 100 K.³⁵ The transient absorption shown in Figure 2 is considered to be due to the T-T absorption of HBT. When the volume fraction of EtOH is small, the peak around 510 nm predominates over the one around 430 nm. As the volume fraction of EtOH increases, the relative composition is reversed. This observation clearly indicates that there are two triplet species of HBT in EtOH + Tol and the proportion depends on the volume fraction of EtOH.

Parts a and b of Figure 3 show the transient absorption spectra of MBT in EtOH + Tol (9:1 volume ratio) and of NBT in DEE + IP (1:1 volume ratio) at 77 K, respectively. A peak can be seen around 430 nm in the spectrum of MBT, while that of the NBT shows a peak around 530 nm. The correspondence of the spectra is considered to reflect a similarity in electronic structure. From Figures 2 and 3, it is thus considered that the electronic structures

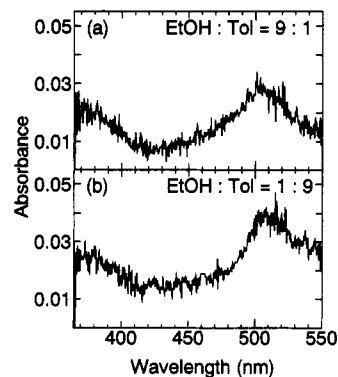


Figure 4. Transient absorption spectra of MHBT obtained at 10 μ s after photoexcitation in EtOH + Tol at 77 K. (a) EtOH : Tol = 9:1. (b) 1:9.

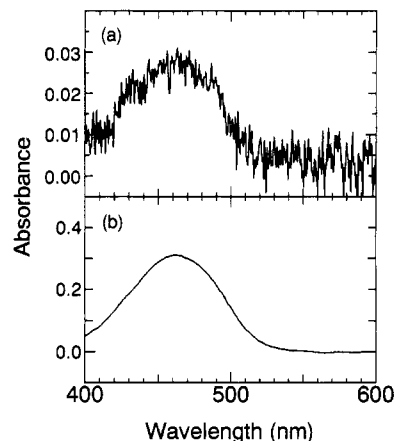


Figure 5. (a) Transient absorption spectrum of HBT obtained at 10 μ s after photoexcitation in DEE + IP (1:1 volume ratio) at room temperature. (b) Steady-state absorption spectrum of NBT in DEE + IP at room temperature.

in the triplet state of HBT in nonpolar and alcoholic solvents are similar to those of NBT and MBT, respectively. Accordingly, the main triplet species of HBT in nonpolar and alcoholic solvents are likely to be an intramolecularly proton-transferred *cis*-keto form and an intermolecularly hydrogen-bonded enol form, respectively. The species in alcoholic solvent will be a *trans*-enol form or an OH rotamer of the *cis*- or *trans*-enol form in Figure 1. When the volume fraction of EtOH is small, the *cis*-keto form predominates over the intermolecularly hydrogen-bonded enol form. As the volume fraction of EtOH increases, the relative composition is reversed. These results are consistent with those obtained from TREPR.⁴² Since the main species in the S_0 state of HBT is a *cis*-enol form in nonpolar solvents, the intramolecular proton transfer is considered to take place in the excited state.

Parts a and b of Figure 4 show the T-T absorption spectra of MHBT in EtOH + Tol (9:1 and 1:9 volume ratios, respectively) at 77 K. In contrast to the case of HBT, these spectra are close to each other and have a peak around 510 nm. From these results, it is considered that the main triplet species of MHBT at 10 μ s after photoexcitation is a *cis*-keto form in both nonpolar and alcoholic solvents. The proportion of the enol form in the triplet state in alcoholic solvents is greatly diminished by the methylation at the 6'-position.

The transient absorption spectrum of HBT obtained in DEE + IP (1:1 volume ratio) at room temperature shows a peak around 460 nm that is not quenched by oxygen (Figure 5a). This transient absorption is thus due to singlet-singlet absorption (S-S absorption). This spectrum is similar to those of HBT in 3-methylpentane and $CHCl_3$ at room temperature.^{35,63} The interpretation of the absorbance decay curves and the lifetime was previously given.^{35,63} The transient S-S absorption spectrum of HBT at room temperature is similar to the steady-state absorption spectrum of NBT shown in Figure 5b. The correspondence of

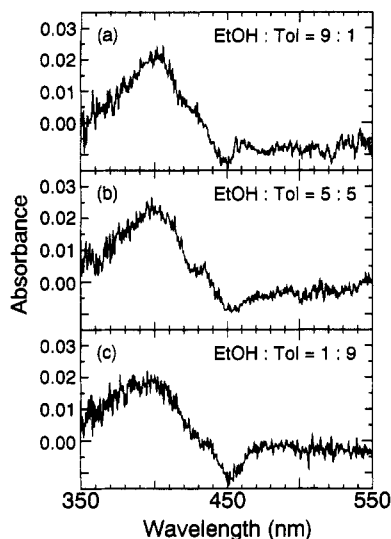


Figure 6. Transient absorption spectra of HBO obtained at 10 μ s after photoexcitation in EtOH + Tol at 77 K. (a) EtOH : Tol = 9:1. (b) 5:5. (c) 1:9.

the spectra is considered to reflect a similarity in electronic structure between NBT and the singlet transient species of HBT at room temperature. Accordingly, it is concluded that the singlet transient species of HBT is a keto form. This result supports the speculation by Al-Soufi et al.³⁵ and Brewer et al.⁶³ that the transient species is a *trans*-keto form. The decay of the triplet species of HBT is likely to occur within the lifetime of the exciting light pulse ($\approx 10 \mu$ s) at room temperature.

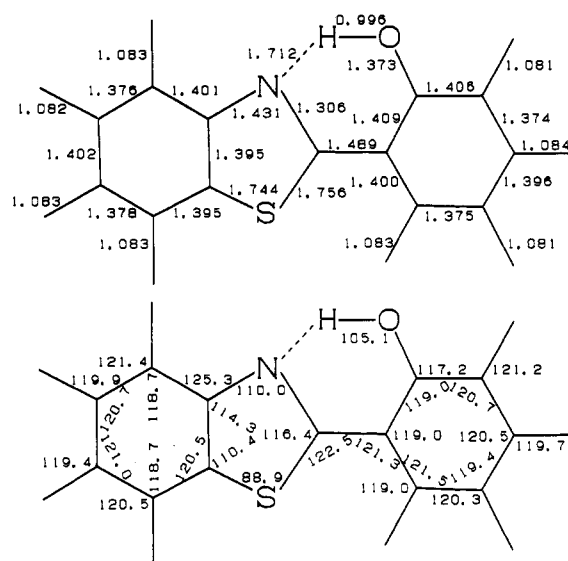
The wavelength of the transient S-S absorption peak for the *trans*-keto form of HBT (460 nm) is close to that of the transient absorption band observed at 77 K (430 nm). It is needed to ensure that the transient absorption band located at 430 nm is due not to the S-S absorption of the *trans*-keto form but to the T-T absorption of the enol form. The transient absorption spectrum of MBT obtained at room temperature is close to that in Figure 3a and shows a peak at 430 nm. The lifetime of the transient species is 125 μ s, and the transient absorption is quenched by oxygen. Accordingly, the transient absorption bands of HBT and MBT located at 430 nm are considered to be due to the T-T absorption of the enol form.

Figure 6 shows the transient absorption spectra of HBO in EtOH + Tol of various volume ratios at 77 K. In contrast to the case of HBT, these spectra are close to one another and have a peak around 400 nm. These spectra are similar to the T-T absorption spectrum of HBO in a mixed solvent of 2-methylpentane and IP (volume ratio 1:1) at 174 K.³⁴ The transient absorption shown in Figure 6 is considered to be due to the T-T absorption. The transient absorption of HBO is negligible at room temperature. The decay of the triplet species of HBO is likely to occur within the lifetime of the exciting light pulse ($\approx 10 \mu$ s) at room temperature.

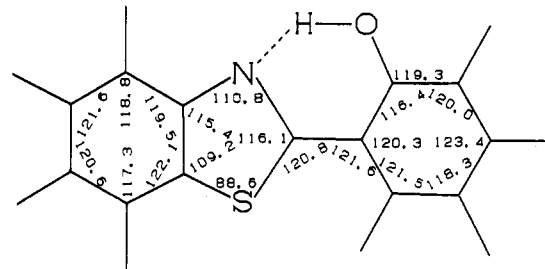
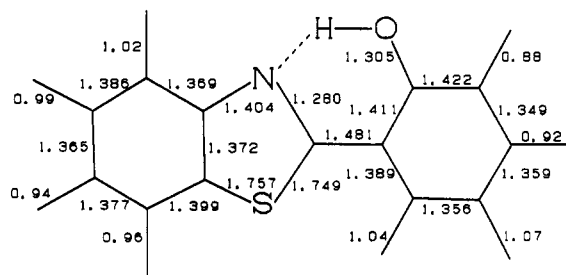
The T-T absorption band of HBO shown in Figure 6 is close to that of the enol form of HBT (Figure 2). It is, thus, considered that the triplet species of HBO at 10 μ s after photoexcitation contain an enol form in both nonpolar and alcoholic solvents. From the results of TREPR,⁴² it was concluded that the main triplet species of HBO at 0.4 μ s after photoexcitation is a *cis*-keto form in both nonpolar and alcoholic solvents. Accordingly, it is considered that the *cis*-keto form produced after photoexcitation is partly converted to the *cis*-enol form in the triplet state within 10 μ s. The conversion process corresponds to proton back-transfer. Actually, both keto and enol forms are in equilibrium at 10 μ s after photoexcitation at 77 K, as shown by Grellmann et al.³⁴

Our assignment of the T-T absorption is also supported by the PPP-type MO calculations. The calculated results of the triplet energies and the *f*-values of the T-T absorption of HBT and HBO are available as supplementary material. Briefly, in the

(a) HBT S₀ Calculated Result



(b) HBT S₀ Experimental Result



(c) HBO S₀ Calculated Result

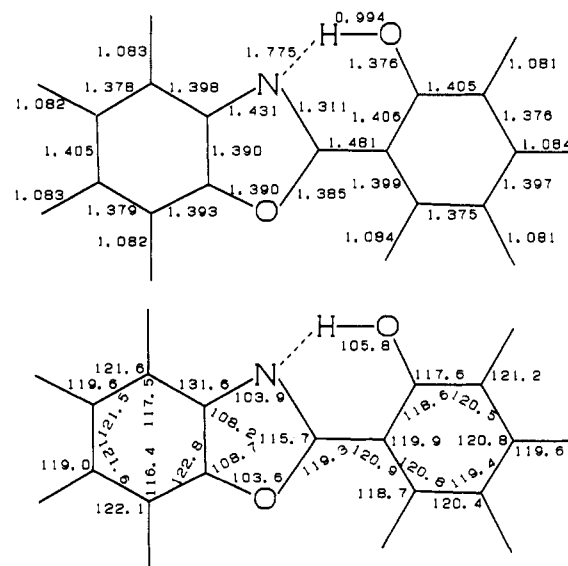


Figure 7. (a) Optimized geometry, in Å and degree, in S₀ state of HBT. (b) Molecular structure of HBT obtained from X-ray diffraction.⁶⁴ (c) Optimized geometry, in Å and degree, the S₀ state of HBO.

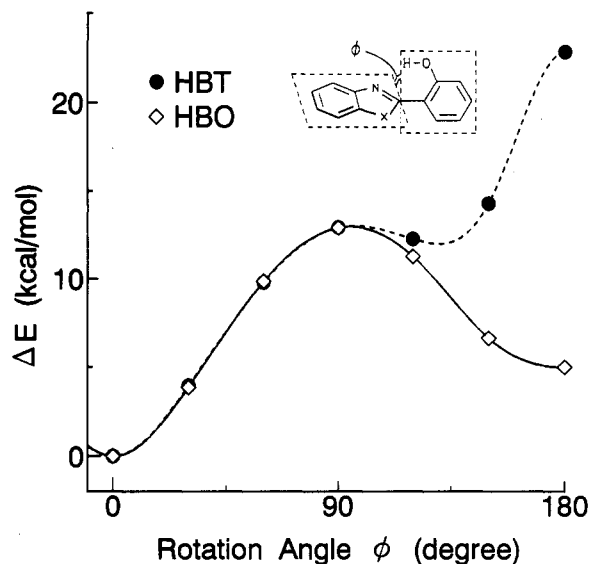


Figure 8. Plots of total molecular energies as functions of dihedral angle $N_3-C_2-C_1-C_2'$ (ϕ) in enol forms of HBT and HBO. The numbers on the ordinate indicate the energy difference (ΔE) from the structure with $\phi = 0^\circ$ (*cis*-enol form).

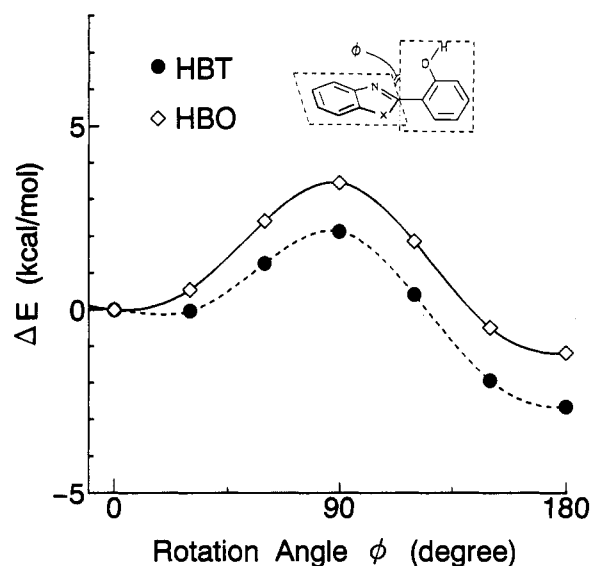


Figure 9. Plots of total molecular energies as functions of dihedral angle $N_3-C_2-C_1-C_2'$ (ϕ) in OH rotamers of enol forms of HBT and HBO. The numbers on the ordinate indicate the energy difference (ΔE) from the structure with $\phi = 0^\circ$ (OH rotamer of *cis*-enol form).

calculated results, the T-T absorption bands in the enol and keto forms of HBT are located at 438 and 446 nm, respectively. Those values for HBO are 398–434 and 438 nm. Although the quantitative agreement between the experimental and calculated results is not sufficient, the calculated wavelength of the T-T absorption band in the enol form is shorter than that in the keto form. The qualitative features of the calculated results are consistent with the experimental ones.

Ab Initio Calculation for the S_0 State. Parts a and c of Figure 7 show the optimized structures (*cis*-enol forms) in the S_0 states of HBT and HBO, respectively. The optimized structure of HBT agrees well with the experimental result (Figure 7b⁶⁴). The $H_{2'}-N_3$ hydrogen bond energies of HBT and HBO were estimated to be 12.4 and 11.0 kcal/mol, respectively. The two energies are similar to each other. The hydrogen bond energy was calculated as the change in total molecular energy in the conversion of the *cis*-enol form (Figure 7a and c) into its OH rotamer (Figure 1).

Figures 8 and 9 show the plots of the total molecular energies as functions of the dihedral angle $N_3-C_2-C_1-C_2'$ (ϕ) for the enol form and its OH rotamer, respectively. In these plots, the numbers

on the ordinate indicate the energy difference (ΔE) from the structure with $\phi = 0^\circ$ (*cis*-enol form in Figure 8 and its OH rotamer in Figure 9). In the calculations for these plots, the geometry parameters other than ϕ were assumed to be the same as those shown in Figure 7a and c. The *trans*-enol form ($\phi = 180^\circ$ in Figure 8) of HBT thus obtained is rather unstable owing to the steric repulsion between $H_{2'}$ and S_1 .

The activation energy for the rotation of the hydroxyphenyl group in Figure 9 contains the energies of the $H_{6'}-S_1$ (O_1) hydrogen bond and of the π -conjugation between the hydroxyphenyl ring and the benzothiazole (benzoxazole) moiety. The activation energy in Figure 8 contains the $H_{2'}-N_3$ hydrogen bond energy besides the above ones. For the *cis*-enol form of HBT and HBO, the activation energies for the rotation of the hydroxyphenyl group are close to each other (Figure 8). For its OH rotamer, the activation energy for HBT is much smaller than that for HBO (Figure 9). For the OH rotamer of HBT (Figure 9), the *trans*-enol form ($\phi = 180^\circ$) is much more stable than the *cis*-enol form ($\phi = 0^\circ$).

When HBT and HBO are intramolecularly hydrogen-bonded in nonpolar solvents (*cis*-enol form), the susceptibilities to rotation of the hydroxyphenyl groups are considered to be close to each other. However, if HBT and HBO are intermolecularly hydrogen-bonded in alcoholic solvents (OH rotamer), HBT is more susceptible to the rotation than HBO. From these calculated results, one can suggest that the *cis*-enol form and the OH rotamer of the *trans*-enol form of HBT exist in the S_0 state in EtOH + Tol. The relative composition depends on the volume fraction of EtOH in EtOH + Tol. In contrast, the main species of HBO in EtOH + Tol is the *cis*-enol form alone. There may be a small amount of the OH rotamer also in HBO, but it will tend to be converted into the *cis*-enol form. These results are consistent with the experimental results described in a previous section and a previous paper.⁴²

Hydrogen Bonding between $H_{6'}$ and S_1 (O_1). The difference in the susceptibilities to rotation of the hydroxyphenyl group between HBT and HBO can be explained in terms of the hydrogen bonding between $C_6-H_{6'}$ and S_1 (O_1). A number of workers postulated that a C-H bond can form an intramolecular hydrogen bond to an ether.⁶⁵ Such a hydrogen bond between $C_6-H_{6'}$ and O_1 keeps HBO planar, even if the other intramolecular hydrogen bond between $O_2-H_{2'}$ and N_3 is absent (OH rotamer of *cis*-enol form). A divalent sulfur atom in a molecule can act as a base in hydrogen bonding.⁶⁵ However, the $H_{6'}-S_1$ hydrogen bond in HBT is much weaker than the $H_{6'}-O_1$ in HBO. The OH rotamer of the *cis*-enol form of HBT is, thus, more susceptible to the rotation of the hydroxyphenyl group than that of HBO.

As described above, the proportion of the triplet enol of HBT in alcoholic solvents is greatly diminished by methylation at the 6'-position. This difference between HBT and MHBT can also be explained in terms of the hydrogen bonding between $C_6-H_{6'}$ [$(CH_3)_6$] and S_1 . In HBT, the ring containing the hydrogen bond is a five-membered one ($C_6-H_{6'}-S_1-C_2-C_1$), while the corresponding ring in MHBT is a six-membered one [$C_6-(CH_3)_6-S_1-C_2-C_1$]. The hydrogen bond in the less-strained⁶⁵ six-membered ring of MHBT will be stronger than that in the five-membered one of HBT. As a result, MHBT is less susceptible to the rotation of the hydroxyphenyl group than HBT in alcoholic solvents, and the proportion of the OH rotamer of the *trans*-enol form in the triplet state is greatly diminished in MHBT.

Ab Initio Calculation for Triplet State. Parts a and b of Figure 10 show the optimized structures in the lowest $^3(\pi, \pi^*)$ states of HBT and HBO, respectively. The initial geometry in the optimization is the optimized geometry of the S_0 state (Figure 7a and c). When we adopt the initial geometry with the $N_3-H_{2'}$ distance shorter than the $O_2-H_{2'}$ one, the triplet energy obtained is much higher than that for the geometry shown in Figure 10. The optimized geometry of the triplet state (Figure 10) is quite different from that of the S_0 state (Figure 7a and c). The C_2-N_3 and C_2-C_1 bond lengths in the triplet state are much longer and

HBT optimized with the AM1 method is nonplanar ($\phi = 28.6^\circ$). This calculated result is not consistent with the experimental one.⁶⁴

Lavtchieva et al. carried out the geometry optimization for the triplet state of HBO with the AM1 method and found that the optimized structure is nonplanar ($\phi = 57^\circ$).⁴⁵ This result obtained with the AM1 method is not consistent with the one obtained with the ab initio method (data not shown); the minimum energy is obtained at $\phi = 0^\circ$ with the ab initio method.

Reliable molecular structures can be obtained with the ab initio method rather than the AM1 method. From these results, it is concluded that the ab initio calculation instead of the semiempirical one is essential for obtaining information about HBT and HBO.

Conclusion

Properties of the $^3(\pi, \pi^*)$ states of HBT and HBO were investigated by means of transient absorption spectroscopy and ab initio calculations. When the volume fraction of EtOH in EtOH + Tol is small, the *cis*-keto form of HBT predominates over the OH rotamer of the *trans*-enol form in the triplet state. However, when the volume fraction of EtOH becomes large, the relative composition is reversed. The triplet species of HBO at 10 μ s after photoexcitation contain a *cis*-enol form in EtOH + Tol. In HBO, the *cis*-keto form produced immediately after photoexcitation is partly converted into the *cis*-enol form in the triplet state within 10 μ s.

Interpretation of the solvent effect was made on the basis of the ab initio calculations for the S_0 state. In the *cis*-enol forms of HBT and HBO, the activation energies of the rotation of the hydroxyphenyl group are close to each other. In the OH rotamer of the *cis*-enol form, the activation energy of HBT is much smaller than that of HBO. Furthermore, in the OH rotamer of HBT, the *trans*-enol form is much more stable than the *cis*-enol form. As a result, the *cis*-enol form and the OH rotamer of the *trans*-enol form of HBT exist in the S_0 state in EtOH + Tol. The relative composition depends on the volume fraction of EtOH. In contrast, the main species in the S_0 state of HBO in EtOH + Tol is the *cis*-enol form alone. The difference in solvent effect between HBT and HBO can be explained in terms of the hydrogen bonding between C_6-H_6 and $S_1(O_1)$.

From the results of the ab initio calculations, it was found that the stable species in the triplet states of HBT and HBO can be regarded as a kind of *cis*-keto form. This result can be explained by considering the π electron nodal pattern of the wave function in the lowest $^3(\pi, \pi^*)$ state.

Acknowledgment. S.N. expresses his sincere thanks to Professor Noboru Hirota of Kyoto University for his valuable discussion. We thank Professor Takuji Ogawa of Ehime University for his valuable discussion of organic syntheses and Professor Jiro Higuchi of Yokohama National University (now professor emeritus) for the use of the program of the PPP method written by him. Our thanks are also due to the Computer Center of the Institute for Molecular Science for the use of the HITAC M-680H and S-820/80 computers and the library program GAUSSIAN 88.⁶¹ This work was partly supported by Grant-in-Aid for Scientific Research (B) No. 03453012 and a Grant-in-Aid on Priority Area "Molecular Magnetism" (Area No. 228/04242104) from The Ministry of Education, Science and Culture of Japan, and by a Grant-in-Aid from the Saneyoshi Scholarship Foundation.

Supplementary Material Available: Calculated results of triplet energies, transition moments, and *f*-values for enol and keto forms of HBT and HBO (Tables I–IV) and molecular structures of HBT and HBO optimized with the AM1 method (Figure 11) (7 pages). Ordering information is given on any current masthead page.

References and Notes

- (1) Klöpffer, W. *Adv. Photochem.* **1977**, *10*, 311.
- (2) Rentzepis, P. M.; Barbara, P. F. *Adv. Chem. Phys.* **1981**, *47* (2), 627.

- (3) Huppert, D.; Gutman, M.; Kaufmann, K. J. *Adv. Chem. Phys.* **1981**, *47* (2), 643.
- (4) Barbara, P. F.; Walsh, P. K.; Brus, L. E. *J. Phys. Chem.* **1989**, *93*, 29 (Future Article).
- (5) *Spectroscopy and Dynamics of Elementary Proton Transfer in Polyatomic Systems*; Barbara, P. F., Trommsdorff, H. P., Eds. *Chem. Phys.* **1989**, *136*, 153–360.
- (6) *M. Kasha Festschrift*; Barbara, P. F., Nicol, M., El-Sayed, M. A., Eds. *J. Phys. Chem.* **1991**, *95*, 10215–10524. Nagaoka, S. *Jpn. Sci. Mon.* **1991**, *44*, 620.
- (7) Nagaoka, S.; Hirota, N.; Sumitani, M.; Yoshihara, K. *J. Am. Chem. Soc.* **1983**, *105*, 4220.
- (8) Chou, P.; McMorrow, D.; Aartsma, T. J.; Kasha, M. *J. Phys. Chem.* **1984**, *88*, 4596.
- (9) Nishiya, T.; Yamauchi, S.; Hirota, N.; Baba, M.; Hanazaki, I. *J. Phys. Chem.* **1986**, *90*, 5730.
- (10) Nagaoka, S.; Hirota, N.; Sumitani, M.; Yoshihara, K.; Lipczynska-Kochany, E.; Iwamura, H. *J. Am. Chem. Soc.* **1984**, *106*, 6913.
- (11) Nagaoka, S.; Fujita, M.; Takemura, T.; Baba, H. *Chem. Phys. Lett.* **1986**, *123*, 489.
- (12) Nagaoka, S. *J. Photochem. Photobiol.* **1987**, *A40*, 185.
- (13) Nagaoka, S.; Nagashima, U.; Ohta, N.; Fujita, M.; Takemura, T. *J. Phys. Chem.* **1988**, *92*, 166.
- (14) Nagaoka, S.; Nagashima, U. *Chem. Phys.* **1989**, *136*, 153.
- (15) Nagaoka, S. *Kagaku to Kogyo (Tokyo)* **1991**, *44*, 182.
- (16) Nagashima, U.; Nagaoka, S.; Katsumata, S. *J. Phys. Chem.* **1991**, *95*, 3532.
- (17) Hoshimoto, E.; Yamauchi, S.; Hirota, N.; Nagaoka, S. *J. Phys. Chem.* **1991**, *95*, 10229.
- (18) Williams, D. L.; Heller, A. *J. Phys. Chem.* **1970**, *74*, 4473.
- (19) Nakagaki, R.; Kobayashi, T.; Nagakura, S. *Bull. Chem. Soc. Jpn.* **1978**, *51*, 1671.
- (20) Mordziński, A.; Grabowska, A. *Chem. Phys. Lett.* **1982**, *90*, 122.
- (21) Ding, K.; Courtney, S. J.; Stranjord, A. J.; Flom, S.; Friedrich, D.; Barbara, P. F. *J. Phys. Chem.* **1983**, *87*, 1184.
- (22) Woolfe, G. J.; Melzig, M.; Schneider, S.; Dörr, F. *Chem. Phys.* **1983**, *77*, 213.
- (23) Itoh, M.; Fujiwara, Y. *J. Am. Chem. Soc.* **1985**, *107*, 1561.
- (24) Elsaesser, T.; Kaiser, W. *Chem. Phys. Lett.* **1986**, *128*, 231.
- (25) Mordziński, A.; Grellmann, K. H. *J. Phys. Chem.* **1986**, *90*, 5503.
- (26) Elsaesser, T.; Schmetzer, B. *Chem. Phys. Lett.* **1987**, *140*, 293.
- (27) Becker, R. S.; Lenoble, C.; Zein, A. *J. Phys. Chem.* **1987**, *91*, 3509.
- (28) Becker, R. S.; Lenoble, C.; Zein, A. *J. Phys. Chem.* **1987**, *91*, 3517.
- (29) Rodríguez Prieto, M. F.; Nickel, B.; Grellmann, K. H.; Mordziński, A. *Chem. Phys. Lett.* **1988**, *146*, 387.
- (30) Nickel, B.; Rodríguez Prieto, M. F. *Chem. Phys. Lett.* **1988**, *146*, 393.
- (31) Elsaesser, T.; Schmetzer, B.; Lipp, M.; Bäuerle, B. *J. Chem. Phys. Lett.* **1988**, *148*, 112.
- (32) Laermer, F.; Elsaesser, T.; Kaiser, W. *Chem. Phys. Lett.* **1988**, *148*, 119.
- (33) Potter, C. A. S.; Brown, R. G. *Chem. Phys. Lett.* **1988**, *153*, 7.
- (34) Grellmann, K. H.; Mordziński, A.; Heinrich, A. *Chem. Phys.* **1989**, *136*, 201.
- (35) Al-Soufi, W.; Grellmann, K. H.; Nickel, B. *Chem. Phys. Lett.* **1990**, *174*, 609.
- (36) Chou, P.-T.; Studer, S. L.; Martinez, M. L. *Chem. Phys. Lett.* **1991**, *178*, 393.
- (37) Frey, W.; Laermer, F.; Elsaesser, T. *J. Phys. Chem.* **1991**, *95*, 10391.
- (38) Grabowska, A.; Sepiol, J.; Rullière, C. *J. Phys. Chem.* **1991**, *95*, 10493.
- (39) Al-Soufi, W.; Grellmann, K. H.; Nickel, B. *J. Phys. Chem.* **1991**, *95*, 10503.
- (40) Eisenberger, H.; Nickel, B.; Ruth, A. A.; Al-Soufi, W.; Grellmann, K. H.; Novo, M. *J. Phys. Chem.* **1991**, *95*, 10509.
- (41) Tero-Kubota, S.; Akiyama, K.; Shoji, F.; Ikegami, Y. *J. Chem. Soc., Chem. Commun.* **1992**, 641.
- (42) Nagaoka, S.; Itoh, A.; Mukai, K.; Hoshimoto, E.; Hirota, N. *Chem. Phys. Lett.* **1992**, *192*, 532.
- (43) Arthen-Engeland, Th.; Bultmann, T.; Ernstring, N. P.; Rodriguez, M. A.; Thiel, W. *Chem. Phys.* **1992**, *163*, 43.
- (44) Chou, P.-T.; Martinez, M. L.; Studer, S. L. *Chem. Phys. Lett.* **1992**, *195*, 586.
- (45) Lavtchieva, L.; Enchev, V.; Smedarchina, Z. *J. Phys. Chem.* **1993**, *97*, 306.
- (46) Nagaoka, S.; Nagashima, U. *J. Phys. Chem.* **1990**, *94*, 1425.
- (47) Nagaoka, S.; Nagashima, U. *J. Phys. Chem.* **1991**, *95*, 4006.
- (48) *Organic Syntheses*; Horning, E. C., Ed.; John Wiley & Sons: New York, 1955; Vol. 3, pp 753–756.
- (49) Cossey, H. D.; Sharpe, C. J.; Stephens, F. F. *J. Chem. Soc.* **1963**, 4322.
- (50) Gray, M.; Parsons, P. J. *Synlett* **1991**, 729.
- (51) Pariser, R. *J. Chem. Phys.* **1956**, *24*, 250.
- (52) Takemura, T.; Hara, K.; Baba, H. *Bull. Chem. Soc. Jpn.* **1971**, *44*, 977.
- (53) Nagaoka, S.; Hirota, N. *J. Chem. Phys.* **1981**, *74*, 1637.
- (54) Nagaoka, S.; Harrigan, E. T.; Noda, M.; Hirota, N.; Higuchi, J. *Bull. Chem. Soc. Jpn.* **1986**, *59*, 355.
- (55) Ohno, K. *Theor. Chim. Acta* **1964**, *2*, 219.
- (56) Klopman, G. *J. Am. Chem. Soc.* **1964**, *86*, 4550.
- (57) Klopman, G. *J. Am. Chem. Soc.* **1965**, *87*, 3300.

- (58) Wolfsberg, M.; Helmholtz, L. *J. Chem. Phys.* **1952**, *20*, 837.
(59) Hinze, J.; Jaffé, H. H. *J. Am. Chem. Soc.* **1962**, *84*, 540.
(60) Dewar, M. J. S.; Morita, T. *J. Am. Chem. Soc.* **1969**, *91*, 796.
(61) Frisch, M. J.; Head-Gordon, M.; Schlegel, H. B.; Raghavachari, K.; Binkley, J. S.; Gonzalez, C.; DeFrees, D. J.; Fox, D. J.; Whiteside, R. A.; Seeger, R.; Melius, C. F.; Baker, J.; Martin, R. L.; Kahn, L. R.; Stewart, J. J. P.; Fluder, E. M.; Topiol, S.; Pople, J. A. *GAUSSIAN 88*; Gaussian, Inc.: Pittsburgh, PA, 1988.
(62) Hehre, W. J.; Radom, L.; Schleyer, P. v. R.; Pople, J. A. *Ab Initio Molecular Orbital Theory*; John Wiley & Sons: New York, 1986.
(63) Brewer, W. E.; Martinez, M. L.; Chou, P.-T. *J. Phys. Chem.* **1990**, *94*, 1915.
(64) Sténson, P. *Acta Chem. Scand.* **1970**, *24*, 3729.
(65) Pimentel, G. C.; McClellan, A. L. *The Hydrogen Bond*; W. H. Freeman and Company: San Francisco and London, 1960.
(66) Grabowska, A.; Mordziński, A.; Tamai, N.; Yoshihara, K. *Chem. Phys. Lett.* **1989**, *153*, 389.
(67) Herek, J. L.; Pedersen, S.; Bañares, L.; Zewail, A. H. *J. Chem. Phys.* **1992**, *97*, 9046.
(68) Peteanu, L. A.; Mathies, R. A. *J. Phys. Chem.* **1992**, *96*, 6910.
(69) Nagaoka, S.; Nagashima, U. 1992 Symposium on Molecular Science, Kyoto, Japan, September 12–15, 1992; 1A19.
(70) Dewar, M. J. S.; Zoebich, E. G.; Healy, E.; Stewart, J. J. P. *J. Am. Chem. Soc.* **1985**, *107*, 3902.